The performance of the WRF-ARW model over Catalonia (NE Spain) with different convective and microphysical parameterizations

Jordi Mercader [(1)], Bernat Codina [(1)], Abdelmalik Sairouni [(2)], Jordi Cunillera [(2)]

(1) Dept of Astronomy and Meteorology, Faculty of Physics, University of Barcelona, Barcelona, Spain

(2) Meteorological Service of Catalonia, Barcelona, Spain

email**: jmercader@am.ub.es**

1. Introduction

Many centers around the world are actively pursuing the development and operational use of the next generation mesoscale modeling system Weather Research and Forecasting (WRF) model (Klemp, 2004).

The performance of the WRF-ARW v2.2 model (Skamarock et al., 2005) has recently been evaluated over Catalonia in order to study the feasibility of being implemented operationally in the Meteorological Service of Catalonia (SMC). Due to the importance of precipitation forecasts in this area, the first goal in this task was to assess the model sensitivity to several configurations of convective and microphysical parameterizations. Our goal is to find a stable configuration, based on an exhaustive verification of standard parameters and on the verification statistics of quantitative precipitation forecasts.

In this work, observational data used to verify the model forecasts and the selected events (several rainfall episodes over Catalonia during 2006-2007) are described in section 2. Next, the model configuration and data used to supply the boundary and initial conditions into the model simulations are explained in section 3, which is followed by the verification methodology in section 4.

Then, the verification results of 36-km and 12-km grid WRF forecasts are presented, for temperature, relative humidity, wind and rain (the latter only for the inner domain).

Here, it is shown how the best results for the coarser domain were achieved with the combination of the Kain-Fritsch convective parameterization and the WSM5 microphysical scheme, whereas in the inner domain the convective parameterization of Kain-Fritsch with the Thompson microphysical scheme yielded the best forecasts. Finally, conclusions and previsions of further work are discussed.

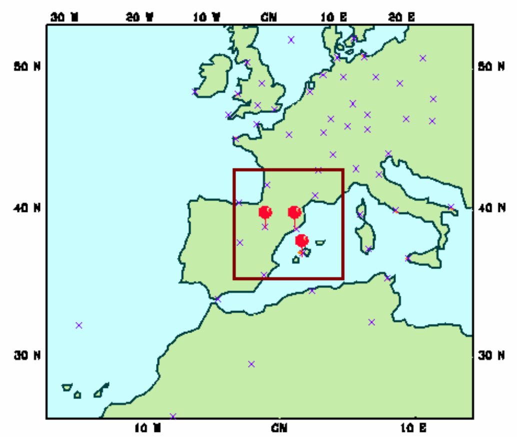

Figure 1. The 36 and 12-km horizontal resolution domains (the latter within the red square), with the radiosounding stations in violet crosses and the three upper-air stations used to verify the inner domain forecasts marked by balloons (from left to right: Zaragoza, Barcelona and Palma de Mallorca).

2. Data description

2.1. Selected events and simulations

For this work, an amount of 602 simulations have been done for 11 selected case studies with rainfall observed over Catalonia, comprised between 15th June, 2006 and 16th March, 2007 (see Table 1). The episodes include both convective and stratiform rainfall while the simulations comprise both 00Z and 12Z initializations.

Case studies (YYYY/MM/DD)	**Number of init. times**	**Number of simulations** (36 km / 12 km)
2006/06/15-16	4	24 / 32
2006/07/05-06	4	24 / 32
2006/08/23-25	6	36 / 48
2006/09/12-16	9	54 / 72
2006/09/24	2	12 / 16
2006/10/11-12	3	18 / 24
2006/10/17-20	7	42 / 56
2007/02/08	2	12 / 16
2007/02/17	2	12 / 16
2007/03/07	2	12 / 16
2007/03/16	2	12 / 16
TOTAL	43	258 / 344

Table 1. List of all the selected case studies, with the number of initialization times associated to each case and the total number of simulations run per case in the coarser / inner domain. A number of 6 (8) configurations for each initialization time have been run for the coarser (inner) domain, resulting from the combination of two microphysical schemes with 3 (4) cumulus parameterizations.

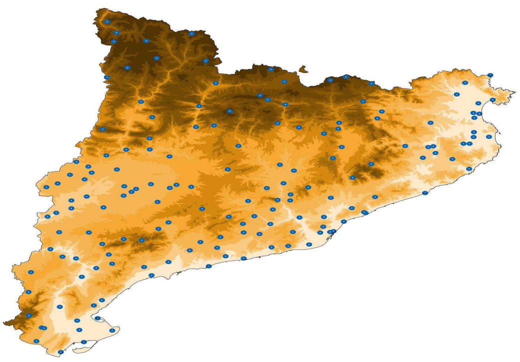

Figure 2. In blue dots, rain-gauges belonging to the SMC network.

2.2. Observational data for verification

In order to perform the verification process for forecasted temperature, relative humidity, geopotencial height, wind and precipitation, the following observational data is used:

- Analyzed field from the Final Analysis product of the GFS model (FNL-GFS)
- Upper observations from the all the radiosounding stations within the domain (see crosses in Figure 1)
- Rain-gauges data of the SMC stations network (Figure 2).

3. Model configuration

Simulations were performed using a set of 2 domains with horizontal grid-point resolutions of 36 and 12 km, both defined as those currently being used for operational forecasts in SMC (RAM, 2007). The coarser domain is a grid of 94x102 points which covers the Southwestern Europe, while the nested inner domain has a grid size of 70x70 points (see Figure 1). Both use the default 31 vertical levels defined in WRF user's manual (Wang et al., 2007).

These simulations have been carried out using the physical and dynamical options displayed in Table 2. The *fixed* options have been kept without change through all the simulations, while the options defined as *tested* schemes, which include cumulus and microphysics parameterizations, have been combined leading to 6 possible combinations of different physical schemes for the coarser domain and 8 available configurations for the inner one. These configurations can be defined as:

- KF.WSM5: Kain-Fritsch (KF) cumulus scheme with the WSM5 microphysics
- KF.Thom: KF scheme with the Thompson microphysics.
- BMJ.WSM5: Betts-Miller-Jánjic (BMJ) cumulus parameterization with the WSM5 microphysics.
- BMJ.Thom: BMJ cumulus scheme with the Thompson microphysics.
- GD.WSM5: Grell-Devenyi (GD) cumulus parameterization with the WSM5 microphysics.
- GD.Thom: GD cumulus scheme with the Thompson microphysics.
- EXP.WSM5: Explicitly resolved convection with the WSM5 microphysical scheme.

- EXP.Thom: Explicitly resolved convection with the Thompson microphysics.

Each simulation has been repeated for each possible configuration in order to evaluate the sensitivity of all these forecasts to each of these possible combinations of cumulus and microphysics schemes.

Initial state and boundary condition data have been supplied by the previous 12-hour initialization of the GFS 1ºx1º-resolution model. In order to improve the first guess, the conventional observations (radiosounding and METAR) have been assimilated through the WRF-3DVAR system (Barker et al., 2004).

Domain	Tested options	Fixed options
36 km	- Cumulus: KF, BMJ and GD - Microphysics: WSM5 and Thompson	- NOAH LSM (4 subsoil layers) - YSU PBL - Monin-Obukhov surface layer - Dudhia and RRTM for SW and LW radiation
12 km	- Cumulus: KF, BMJ, GD and NO convection - Microphysics: WSM5 and Thompson	

Table 2. For each domain, tested and fixed physical options that had been used for the model simulations.

4. Methodology

4.1. Verification of the 36-km domain

The verification in the coarser domain has been done for the forecasted temperature, relative humidity, geopotencial height and wind using two methods:

1) Grid to grid verification: Comparing the forecasted fields with the analysis fields generated by the WRF model, using as a first guess the analyzed fields supplied by FNL-GFS improved by observational data ingested by WRF-3DVAR.
2) Point to point verification: The forecasted values of the same variables in standard vertical levels have been verified against data supplied by upper-air observations. In order to avoid any interpolation, the grid points chosen for comparison are the nearest neighbors of each radiosounding station.

4.2. Verification of the 12-km domain

In the inner domain, the accuracy of temperature, relative humidity and wind forecasts has been evaluated using vertical observational data from 3 radiosounding stations: Barcelona, Palma and Zaragoza (Figure 1).

Moreover, the verification of quantitative precipitation forecasts (QPF), based on traditional statistics indexes obtained from the model field against observations in form of analysis have been computed. Rain is actually the variable that concerns most in this work.

In order to build the best observed rainfall field, an analysis of rainfall observations has been done over a 32x24 grid over Catalonia, where the forecasted rainfall has also been interpolated to. Afterwards, a mask has been applied to both analyzed and forecasted fields in order to compare only the area within Catalonia boundaries.

Using these masked fields, two dimensional contingency tables were built for several rainfall intensity thresholds, considering the 4 possible pairs of YES/NO observations and forecasts. Then, some statistics, such has POD, FAR, BIAS and CSI are derived from the table parameters.

5. Results

5.1. 36-km domain

In this section, the results of the comparison of the forecasted standard parameters (temperature, relative humidity, geopotencial and wind) against the analysis from the same model, as well as the results from the forecasted against the observed radiosounding verification are discussed.

In general, the temperature forecast errors increase with forecast length (not shown) but decrease with height (see Table

3), except between the upper levels (500 and 300 hPa). This variable is underestimated in the lowest levels while it is overestimated in 300 hPa. The configurations with better results are those that use the KF cumulus scheme (not shown).

Geopotencial height tends to be underestimated (see Table 3). The best results of the S1 score (not shown) are given by the KF.WSM5 configuration.

On the other hand, the mean vector wind error (MVWE) index gives very similar results between all the configurations (see Table 3).

	LEV (hPa)	KF. WSM5	KF. Thom	BMJ. WSM5	BMJ. Thom	GD. WSM5	GD. Thom
T (ºC)	**850**	**-0.18** **(1.27)**	-0.24 (1.30)	-0.32 (1.31)	-0.28 (1.31)	-0.30 (1.33)	-0.28 (1.34)
	700	-0.09 **(0.97)**	**-0.08** **(0.97)**	-0.20 (0.99)	-0.17 (0.98)	-0.12 (0.98)	-0.09 (0.98)
	500	-0.03 (0.92)	-0.03 **(0.91)**	+0.02 (0.93)	**+0.01** (0.92)	**-0.01** (0.93)	**-0.01** (0.92)
RH (%)	**850**	**+0.1** (13.5)	+1.2 (13.6)	**-0.1** **(13.1)**	-0.2 (13.2)	+0.2 (14.5)	+0.4 (14.5)
	700	-1.1 (16.6)	-0.7 (16.5)	-0.3 **(16.4)**	**-0.2** (16.5)	-1.5 (17.1)	-1.4 (17.2)
	500	**-0.4** **(19.9)**	**+0.4** (20.0)	+1.6 (20.6)	+2.3 (20.8)	-1.2 (20.1)	-0.7 (20.2)
Z (m)	**850**	-4.4 (11.7)	-4.5 (11.7)	**-3.8** (11.6)	**-3.8** **(11.2)**	-4.4 (11.8)	-4.6 (11.9)
	700	**-5.3** **(12.1)**	-5.5 (12.3)	-5.9 (12.6)	-5.5 **(12.1)**	-5.6 (12.5)	-5.7 (12.5)
	500	**-5.6** (14.3)	-5.7 (14.4)	-6.3 (14.6)	-5.9 **(13.9)**	-5.9 (14.5)	-6.0 (14.5)
WIND (m/s)	**850**	**4.01**	4.02	4.09	4.09	4.04	4.04
	700	**3.82**	3.84	3.87	3.87	3.86	3.87
	500	4.11	4.11	4.13	4.12	4.11	**4.10**

Table 3. ME (and RMSE) of temperature, relative humidity and geopotencial height and MVWE of wind for 24-hr forecasts initialized at 00Z, corresponding to grid to grid verification over the 36-km domain. The best results are marked in bold.

Finally, the verification results of relative humidity give more unbiased forecasts in lower levels than in upper levels, where all the simulations tend to be moister (see Table 3 and Figure 3). It can be also seen that configurations with the BMJ cumulus scheme are the driest in lower levels and the moistest in upper levels. Concerning to the RMSE index, it tends to increase with height (see Figure 3 and Table 3), but differences between configurations are too little to decide which of them gives the best results.

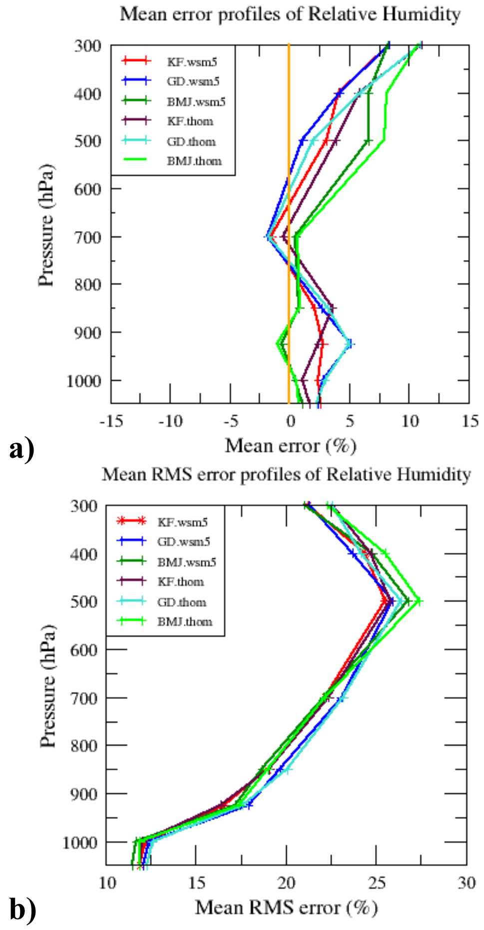

Figure 3. Vertical profiles of point to point (a) ME and (b) RMSE of relative humidity computed over all the radiosounding stations within the 36-km domain.

5.2. 12-km domain

Firstly, the forecasted and observed radiosounding profiles for the conventional variables have been compared in three points within the inner domain (Figure 1). Then, the verification statistics have been applied to QPF.

5.2.1. Conventional variables

Generally, the ME and RMSE values for temperatures are low in all vertical profiles. The variable is usually overestimated in upper levels, while the behavior in lower levels depends on the site. The configurations with the GD and KF cumulus schemes behave more regularly than the others (not shown).

For the wind, the MVWE in lower and upper levels tend to be higher than in medium levels. The configurations with best forecasts are those using the KF and BMJ schemes (not shown).

In addition to this, the verification of relative humidity shows that ME (Figures 4a-6a) is low (-10, 15 %) in the three sites and for all levels. In Barcelona and Palma, the model is moist in lower levels and very moist in upper levels; however, in Zaragoza the whole vertical profile is too moist. On the other hand, the RMSE (Figures 4b-6b) tend to increase with height in lower levels, while from the 500 to 300 hPa it tends to decrease in Barcelona and Palma.

Finally, it can be noted that almost all the configurations give similar verification results, except the combination of explicitly resolved convection with the Thompson microphysical scheme, that provide worse results.

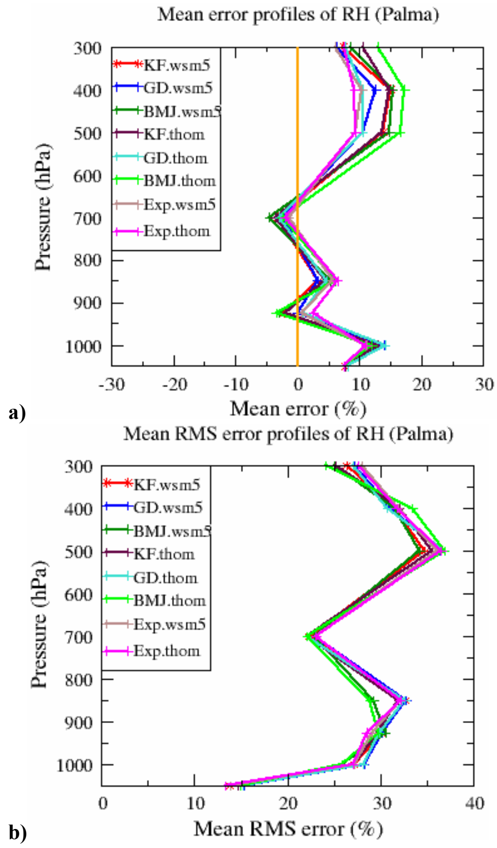

Figure 5. Vertical profiles of (a) ME and (b) RMSE for RH in Palma.

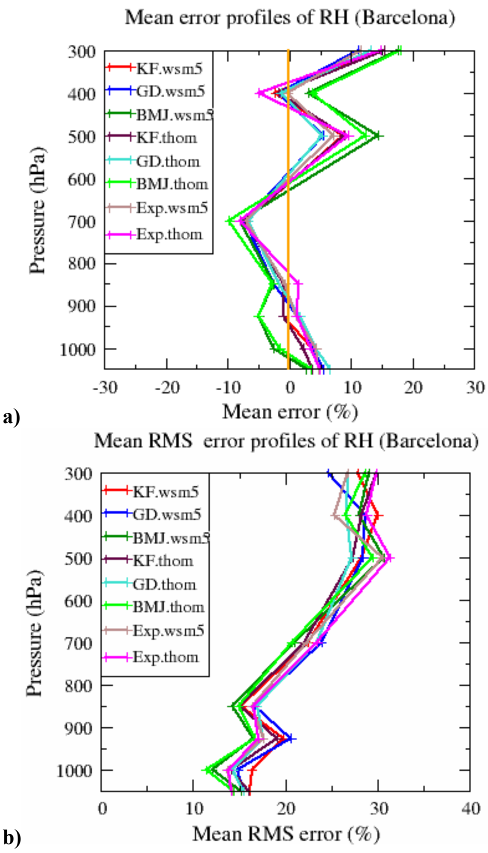

Figure 4. Vertical profiles of (a) ME and (b) RMSE for RH in Barcelona.

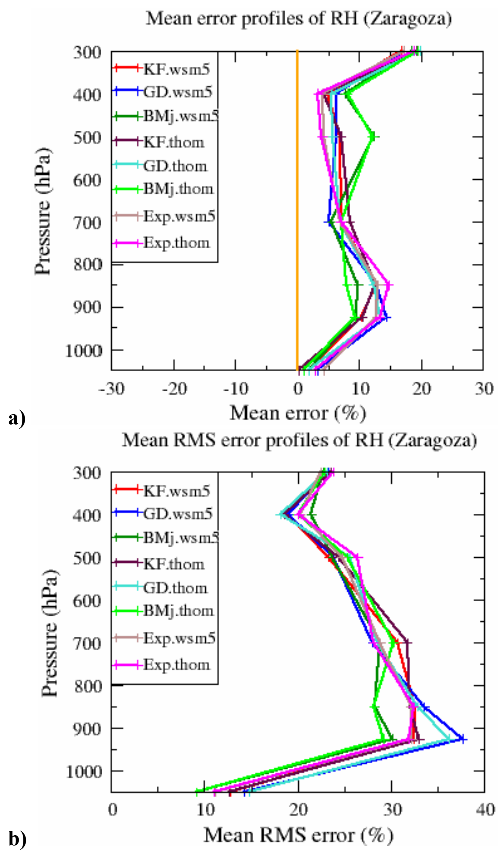

Figure 6. Vertical profiles of (a) ME and (b) RMSE for RH in Zaragoza.

5.2.2. QPF verification

The first objective of this verification is to select the best configurations among all the eight in order to study them more carefully.

The first to be discarded are the configurations with the BMJ convective schemes, because they show to be useless for high intensities. In fact, these configurations tend to do good forecasts of less intense precipitation events, but usually miss the most intense episodes (see Table 4).

In contrast, such configurations that resolve convection explicitly have a poor skill for lower intensity thresholds, but they are able to give the best forecasts for some events of high intensity (see Table 4). However, they usually overestimate the frequency of such episodes and their false alarm ratio can be high. Then, they can be considered useful for the most extreme events, but only the configuration with the WSM5 scheme is chosen, because the other has shown the worst performance in conventional variables.

The other configurations, with the KF and GD cumulus schemes, do not have their optimal behavior as biased as those mentioned before. In fact, it is difficult to decide which of the four configurations that use the KF and GD cumulus schemes perform best, but only those combined with the Thompson microphysics scheme are chosen because their results are very similar but slightly better than configurations with the WSM5 scheme (see Table 4).

	KF. wsm5	KF. Thom	BMJ. wsm5	BMJ. Thom	GD. wsm5	GD. Thom	EXP. wsm5	EXP. Thom
CSI	0.32 **0.07**	**0.33** **0.07**	0.32 0.03	**0.33** 0.03	0.30 **0.07**	0.31 **0.07**	0.24 0.05	0.24 **0.07**
POD	**0.53** 0.23	**0.53** 0.23	0.51 0.10	0.52 0.10	0.49 0.22	0.49 **0.25**	0.38 0.15	0.35 0.18
FAR	0.53 0.79	0.52 0.79	0.52 0.52	0.51 0.55	0.48 0.68	0.51 0.68	0.54 0.73	0.44 0.72

Table 4. Values of CSI, POD and FAR scores calculated for the precipitation intensity threshold of 3 mm/6h (upper values) and 10 mm/6h (lower values) corresponding to the 00Z simulations valid at +18h hour. The highest values of CSI and POD are in bold.

The temporal evolution of POD and CSI scores display two maximum values over the 18 and 36 hours length of forecast (see Figures 7 and 8). Taking into account that simulations were initialized at 00Z, these hours correspond to the 12Z-18Z interval of the first day and the 6Z-12Z interval of the second day, which are the times of the day when most convective activity is observed in the area.

On the other hand, the comparison of the three configurations displays that the KF.Thom have a better skill than the GD.Thom at almost all forecast hours (see Figure 7 and 8) because the POD index is higher and the FAR index is lower, leading consequently to a higher CSI score. However, both configurations show that in periods when the POD and CSI scores increase, the FAR index decreases, a fact which demonstrates a good performance of the rain forecasts.

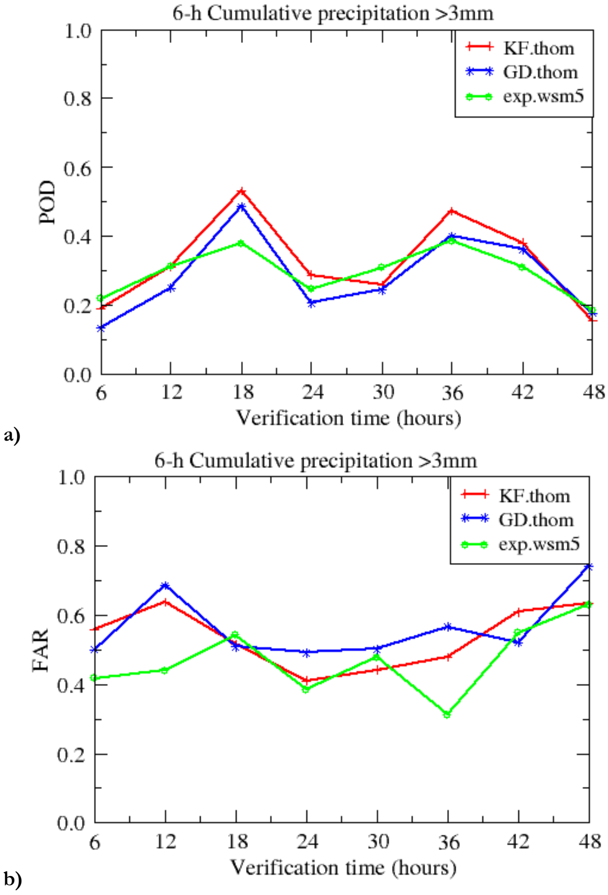

Figure 7. Temporal evolution of (a) POD and (b) FAR scores, averaged over all simulations initialized at 00Z, for the three chosen configurations, corresponding to the 6-h accumulated QPF > 3 mm.

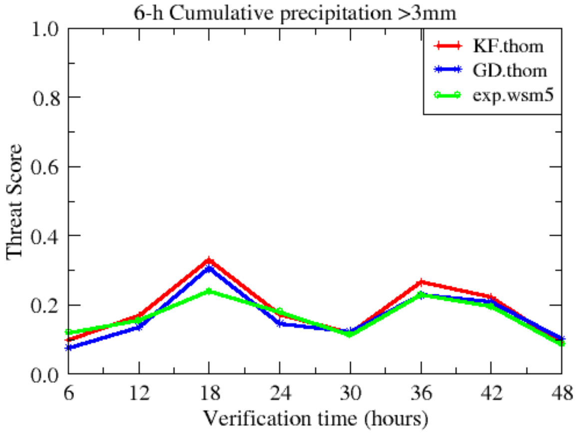

a)

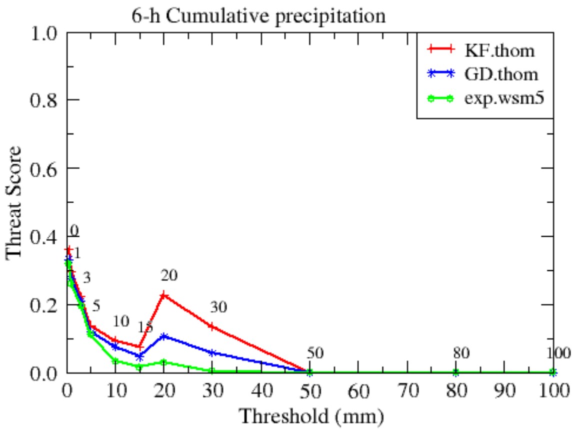

b)

Figure 8. a) Temporal evolution of the CSI score averaged over all simulations initialized at 00Z, for the three chosen configurations, corresponding to the 6-h accumulated QPF > 3 mm. **b)** The CSI score averaged over all simulations initialized at 00Z, in function of the intensity threshold, for the 36-42h forecast length interval, corresponding to the afternoon of the second day of forecast.

Interestingly, the configuration with explicitly resolved convection gives the best CSI and POD indexes during the night, while it tends to produce the poorest performance in daytime hours.

Since afternoon is the period in which the most convective activity is usually observed, it is interesting to analyze the comparative performance of these configurations during a 6-hour interval in such a time of the day, as it is displayed in Figure 8b. It is clearly seen that, while for lower precipitation thresholds (less than 5 mm) all the configurations have a similar skill, the KF.Thom configuration shows the best performance for higher amounts of precipitation.

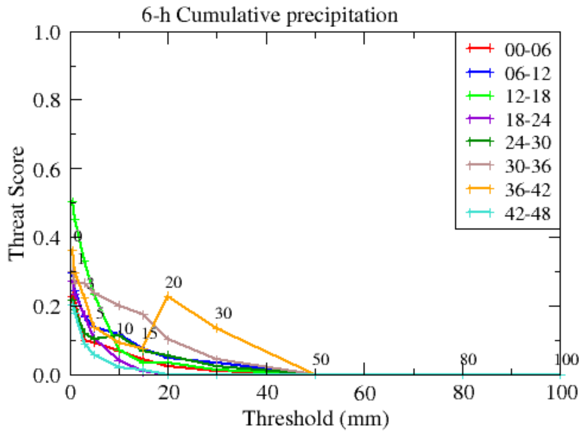

Figure 9. For the model configuration with KF and Thompson, CSI score averaged over all simulations initialized at 00Z, for each 6-hour forecast length interval in function of the accumulation threshold.

The analysis of the results indicates that all combinations show a considerable forecast skill, but the combination of the Kain-Fritsch convective parameterization with the Thompson microphysical scheme demonstrates to have the best forecast skill and the most consistent behavior.

Using this configuration, the CSI score displayed in function of the intensity threshold for each of the 6-hourly intervals (Figure 9) indicate the best performance between 12 and 18 UTC of the first day with light precipitation, between 06 and 12 UTC of the second day when QPF is moderate, and between 12 and 18 UTC of the second day if the forecasted rainfall is heavier.

6. Conclusions

In this work, the sensitivity of the WRF-ARW 2.2 model to combinations of the different cumulus parameterizations available in this model with the WSM5 and Thompson microphysical schemes has been evaluated. The main purpose was to find a stable configuration for the model for operational forecasts in SMC.

For both domains, verification of the conventional variables has been done through the computation of the ME and RMSE indexes and the MVWE for the wind. The best results for the coarser domain have been done by the KF.WSM5 configuration, while for the inner domain only it has been concluded that the EXP.Thom configuration shows the worst skill.

Moreover, for the inner domain, the QPF has been verified using classical statistic scores. The analyses of the results show that the KF.Thom configuration has the best skill for QPF.

These two configurations (KF.WSM5 for the coarser domain and KF.Thom for the nested) will be used for operational forecasts in SMC. Then, the WRF forecasts will be verified against the other models that are currently operationally run in SMC (MM5, MASS and Lokal Modell).

Acknowledgements

We would thank help and advice given by J.R. Miró, M. Pagès, J. Toda, M. Aran, M. Bravo, T. Barrera, J. Moré and C. Antón, from the Applied Research and Modeling team of SMC.

References

Applied Research and Modeling Area, Meteorological Service of Catalonia (RAM-SMC), 2007. Verificació dels models de mesoescala operatius al SMC (Verification of mesoscale operational models in SMC). Notes d'Estudi del SMC – núm. 71.

Barker, D. M., W. Huang, Y. R. Guo, and Q. N. Xiao., 2004**.** A Three-Dimensional (3DVAR) Data Assimilation System For Use With MM5: Implementation and Initial Results. *Mon. Wea. Rev*., **132**, 897-914.

Klemp, J. B., 2004**:** Next-Generation Mesoscale Modeling: A technical overview of WRF. Presentation at the 20th Conference on Weather Analysis and forecasting and 16th Conference on Numerical Weather Prediction. Seattle, WA, 11-15 January 2004.

Skamarock, W. C., Klemp, J. B., Dudhia, J., Gill, D. O., Barker, D. M., Wang, W., and Powers, J. G., 2005 (revised 2007): A description of the Advanced Research WRF Version 2. NCAR Tech Notes-468+STR.

Wang, W., Barker, D., Bray, J., Bruyère, C., Duda, M., Dudhia, J., Gill, D., Michalakes, J., 2007**.** User's Guide for Advanced Research WRF (ARW) Modeling System Version 2.2. Mesoscale and Microscale Meteorology Division - National Center for Atmospheric Research (MMM-NCAR).